A Psychological Approach for the Path Planning of Human Evacuations in Contaminated Indoor Environments

Amanda C. Dings * **Constantina M. Gatsonis** * **Michael A. Demetriou** *

* *Worcester Polytechnic Institute, Worcester, MA 01609 USA (e-mail: {adings,cmgatsonis,mdemetri}@wpi.edu).*

Abstract: This work considers a level-set based algorithm for guiding evacuees in indoor environments. The algorithm considers the accumulated inhalation of a hazardous substance such as carbon monoxide and attempts to provide an optimal path to ensure survivability. The algorithm also considers psychological decision making of evacuees. The most significant psychological contribution to overall evacuation time is the tendency of evacuees to underreact, causing decision making delays. During an emergency, evacuees with high risk perception will be directly incentivized to make evacuation decisions, while those with low risk perception will likely continue to delay decision making. This work models this phenomenon by simulating an initial accumulated concentration before the evacuee begins moving. Earlier work has shown that level-set based paths are much more likely to lead an evacuee to safety than a constant angle path, because they ensure the evacuee's peak exposure to the hazardous substance remains low. After including the psychological delay, this work supports these results. Additionally, a higher initial concentration (i.e. a longer psychological delay) decreases the chances of survival more significantly than does a higher instantaneous concentration of the field itself.

Keywords: Level-set path planning; indoor evacuation; spatially varying fields; psychological effects.

1. INTRODUCTION

Evacuation of enclosed spaces during building fires and chemical emergencies has been the subject of earnest research in the fields of fire protection engineering, psychology and sociology. It is thanks to these research communities that policies have been put in place by agencies such as the United States Federal Emergency Management Agency (FEMA) to ensure safety during evacuations (e.g., building codes, exiting procedures, readiness awareness programs, etc.) (ICC, 2014). However, these initiatives by and large may not take into account the chemical byproducts of fire–such as carbon monoxide (CO)–and how these byproducts may affect the survivability of potential exit paths.

This work attempts to address the issue of CO survivability in an evacuation environment by considering both the *psychological factors* which affect human behavior during evacuations, as well as the *physiological factors* which affect human movement and survivability in evacuations.

1.1 Psychological Factors

Small scale evacuation refers to sudden and relatively localized emergencies, such as a fire outbreak or building collapse. Evacuation of such events occurs on foot. They differ from long-distance regional evacuations, which result from events such as earthquakes, and often involve vehicles as transport (Li et al., 2014). The former will be our primary focus here.

A general set of human reactions prior to evacuation has been identified throughout literature. This time period, beginning with the first emergency cue and ending with the movement towards exits, is known as *pre-evacuation* (Zhao et al., 2009). The pre-evacuation period can be further broken down into three parts: (i) the *pre-alarm phase*, (ii) the *information seeking phase*, and (iii) the *response phase* (Kinateder et al., 2015). The decisions made during this stage have significant effect on the overall pre-evacuation time (Zhao et al., 2009).

The pre-alarm phase refers to period prior to and including the first emergency cue, i.e. smoke, debris, an alarm, etc. (Kinateder et al., 2015). Following the first sign of emergency, the first psychological choice of action is to investigate further in order to either confirm or deny that there is in fact an emergency (Wang et al., 2016; Zhao et al., 2009; Mu et al., 2013). This marks the beginning of the information seeking phase and is likely due to the dislike of ambiguity (Mu et al., 2013). It is also affected by the degree of perceived risk and is further discussed below (Waldau et al., 2005). The second choice of action is to discuss the nature of the event or to alert others of an emergency (Zhao et al., 2009). Finally, decisions regarding evacuation are made in the response phase, during which an individual will take protective actions, which include evacuation or seeking shelter in place (Kinateder et al., 2015).

Made evident through evacuation delays in the pre-evacuation phase is the tendency for humans to under-react in potentially hazardous situations (Drury and Cocking, 2007). Fire injury and death research has found that over two-thirds of the injured and over half of the dead in building fires could have evacuated, but instead engaged in behaviors that delayed their exit (Kuligowski, 2017). The notion of widespread panic during emergencies, though popularized through media, is seldom seen in actual evacuation or emergency scenarios (Drury and Cocking, 2007; Zhao et al., 2009). Freezing behavior often occurs in individuals during an emergency, which further in-

★ The authors gratefully acknowledge financial support from DARPA, DSO-Lagrange grant # 214355 and NSF-CMMI grant # 1825546.

creases evacuation delays (Leach, 2004; Drury and Cocking, 2007). This passivity in the face of danger is attributed to difficulty processing the reality of their situation, resulting in this reflexive reaction (Leach, 2004). Moreover, freezing can be considered a coping mechanism (Drury and Cocking, 2007). Therefore, the psychology of decision making in such an event is likely more informative in regard to the total evacuation time, which includes the pre-evacuation stage and the final act of evacuating, than factors such as building design, i.e. exit width and travel distance (Drury and Cocking, 2007). Delaying *evacuative actions* can take longer than the time necessary to travel the distances to and through exits (Vorst, 2010).

Evacuation delays also serve as a buffer during which an individual will work to assess and confirm the warning cues (Kuligowski, 2017). As previously discussed, this is achieved through information seeking behaviors. More ambiguous cues result in a higher probability that individuals will search for information (Kuligowski, 2017). Information obtained during this time, as well as the cues themselves, heightens the recipient's perceived risk. This is because experiencing warning cues associated with emergency make dismissing the situation more difficult and obtaining information makes the event's severity known, thus increasing perceived risk (Kuligowski, 2017).

Risk perception is one of the most prominent factors affecting human decision making during the pre-evacuation period. Research and interviews with survivors from the September 11, 2011 attacks on the World Trade Center indicated a positive correlation between perceived risk and protective evacuation decisions. Seventy percent (70%) of the building's occupants reported that feeling at risk pushed them to make an evacuation decision. Similarly, lower perceived risk was linked to evacuation delays (Kinateder et al., 2015). Thus, risk perception is considered to directly influence protective decision-making, as well as the direction and strength of the relationship between the predictor variable and the protective action (Kinateder et al., 2015). Additionally, a curvilinear relationship exists between perceived risk and information seeking behaviors; if extremely high or low, individuals are less likely to investigate the emergency (Kinateder et al., 2015).

1.2 Physiological Factors

A multitude of physiological factors affect an evacuee's effectiveness in escaping areas where hazardous amounts of CO are liberated, such as building fires (Gozubuyuk et al., 2017). Some of these factors include *age*, *bodily size*, and *physical conditions* such as cardiac stability, aerobic fitness, and bodily mobility (Gozubuyuk et al., 2017). Furthermore, health conditions such as emphysema and asthma will lower respiratory capacity (Gozubuyuk et al., 2017). Age also plays a role in evacuation efficiency; young adults are generally able to walk more quickly than children and the elderly. Additionally, men walk faster than women. An ideal path planning algorithm will consider in detail physiological factors such as these. For the sake of simplicity, this work does not consider these factors individually. However, it attributes the pre-existing accumulated amount of CO due to both evacuative action such as evacuation delays, and physiological factors.

While the physiological factors that affect the evacuee's ability to escape vary greatly between individuals, the susceptibility of humans to CO exposure is well documented and may be generalized across the human population. According to the National Fire Protection Association, the concentration of CO–measured in parts per million (ppm)–is a determining factor of the symptoms of an average adult (National Fire Protection Association, 2008). The symptoms of CO poisoning can be predicted based on the percentage of CO in the bloodstream (Gozubuyuk et al., 2017). According to Permentier et al. (2017), percentages less than 5% cause little to no toxicological effects. However, CO percentages between 41% and 50% can cause loss of consciousness in seconds (Gozubuyuk et al., 2017). According to Demetriou and Kontopyrgos (2019a), the safe limit of CO inhalation is based on the peak concentration already sustained. If an individual has encountered a high peak CO concentration, then their safe limit of exposure is drastically reduced. If the same individual avoids high peak exposure, they will have a higher limit for accumulated exposure.

1.3 Previous Work and Contributions

Previous work in this field has provided insight into the effects of CO exposure on the human body. Coşkun et al. (2019) proposes that CO exposure time is positively correlated to the concentration of carboxyhaemoglobin, a chemical which impairs oxygen transport. Demetriou and Kontopyrgos (2019a) also propose a model for CO poisoning. If an individual has sustained a peak CO concentration in excess of 2,000 ppm, then the safe limit of accumulated exposure for this individual is $c_{thresh} = 25,000$ ppm. Conversely, the safe limit of accumulated exposure for peak CO concentrations less than 2,000 ppm is $c_{thresh} = 64,000$ ppm. This is the model for CO poisoning that will be used for this work.

Earlier work in this field has proposed a model for evacuee survival that includes instantaneous (peak) CO concentration as well as accumulated concentration. It has been demonstrated by Demetriou and Kontopyrgos (2019a) that in such a model, a straight-angle path may not be survivable, while a level-set approach might be. The current work attempts to replicate this result, while taking into account a brief psychological delay incurred during the pre-evacuation phase.

The current work aims to contribute the effects of an initial concentration inhaled on the survivability of a candidate evacuation path. Such an initial accumulated concentration (amount of CO inhaled in lungs) stems from the evacuation delay whereby the evacuee, due to the psychological factors takes no action while inhaling and accumulating CO in the lungs. The effects of initial concentration versus field intensity are analyzed so as to determine a relationship between field concentration, initial concentration due to delayed evacuative action, and survivability for both constant angle and level-set based paths.

The remainder of this paper is as follows. Section 2 describes the mathematical method used to solve the aforementioned problem. Section 2.1 summarizes the mathematical model of CO field. Section 2.2 describes the kinematic equations modeling the motion of a single evacuee during an evacuation procedure. Section 2.3 presents the accumulation model due to inhalation of CO. Section 2.4 states the path planning (control) problem and Section 2.5 describes the path planning algorithms used. Section 3 presents the results of the numerical studies, and Section 4 discusses conclusions and areas for future work.

2. PROBLEM FORMULATION AND MAIN RESULTS

2.1 Mathematical modeling of spatial field

The dispersion of hazardous substance, such as the CO, is assumed to be governed by an advection-diffusion partial differential equation (PDE), (Seinfeld and Pandis, 1997; Arya, 1999). Assuming multiple sources of the species, the dispersion equation is given, in its general form by the PDE in a 3D rectangular spatial domain $\Omega = [0, L_\chi] \times [0, L_\psi] \times [0, L_\zeta]$, by

$$\frac{\partial c}{\partial t} = \nabla \cdot (D\nabla c) - \nabla \cdot (uc) + \sum_{i=1}^{n} b_i f_i \tag{1}$$

where $c(t, \chi, \psi, \zeta)$ denotes the species concentration at time $t \in \mathbb{R}^+$ and spatial coordinates $(\chi, \psi, \zeta) \in \Omega$, D the (eddy) diffusivity, u the wind velocity vector and $b_i = b_i(\chi, \psi, \zeta)$, $i = 1, \ldots, n$ the spatial distribution of the source terms and $f_i = f_i(t)$, $i = 1, \ldots, n$ their corresponding temporal component; i.e. $f_i(t)$ denotes the mass release rate. The above is furnished with boundary and initial conditions

$$c(0, \chi, \psi, \zeta) = c_0(\chi, \psi, \zeta), \qquad c|_{\partial\Omega_1} = 0, \quad \nabla c_{\partial\Omega_2} = 0, \tag{2}$$

where the mixed conditions are assumed for the boundary $\partial\Omega = \partial\Omega_1 \times \partial\Omega_2$. Equations (1), (2) can be simplified to their steady-state representation, thereby arriving at Poisson's PDE.

Following the assumption argued in (Demetriou and Kontopyrgos, 2019b), the 3D PDE representing the species dispersion in an indoor environment can be reduced to a 2D PDE by assuming axisymmetry in the vertical direction; this stems from the fact that the vertical variation of the concentration field around the head of an average human is negligible compared to the variation across the horizontal plane. The 2D PDE can be further simplified if the time scales involved (total evacuation duration and PDE time constant) are not of the same order. This reduces the 2D advection-diffusion PDE to 2D Poisson's equation. In its simplest form Poisson's equation is

$$\Delta c = g, \quad c|_{\partial\Omega_1} = 0, \quad \nabla c_{\partial\Omega_2} = 0, \tag{3}$$

where the Laplace operator is $\Delta\varphi = \varphi_{\chi\chi} + \varphi_{\psi\psi} + \varphi_{\zeta\zeta}$ for $\varphi \in H_0^1(\Omega)$ and $g \in H^{-1}(\Omega)$ encompasses the spatial distribution and strength of all n sources in (1).

Since each evacuee has access to the full state $c(\chi, \psi)$ in (3), then the concentration at the coordinates $(x, y) \in \Omega$ of the evacuee is given by

$$\gamma = \int_0^{L_\chi} \int_0^{L_\psi} \delta(\chi - x)\delta(\psi - y)c(\chi, \psi)\mathrm{d}\psi\mathrm{d}\chi = c(x, y).$$

When the evacuee is moving, the coordinates are given by $(x(t), y(t))$ and the above becomes a time-varying function

$$\begin{aligned}\gamma(t) &= \int_0^{L_\chi} \int_0^{L_\psi} \delta(\chi - x(t))\delta(\psi - y(t))c(\chi, \psi)\mathrm{d}\psi\mathrm{d}\chi \\ &= c(x(t), y(t)).\end{aligned} \tag{4}$$

This can be viewed as the output of a sensor placed at the evacuee's coordinates and having a spatial distribution given by the spatial delta function centered at $(x(t), y(t))$.

The CO field used here is assumed to be governed by the 2D Poisson's PDE in (3) with a known source location and strength. As such, a gaussian distribution is used as its solution with a χ- and ψ-covariance S_χ and S_ψ, and centered at location (C_χ, C_ψ) (source location). Thus, the CO concentration is given in (5) below, where the constant K may be altered to change the field intensity. Fig. 1 is included to visualize the spatial field.

$$c(\chi, \psi) = 4.1 \times 10^4 K \mathrm{e}^{\left(-\left(\frac{(\chi - C_\chi)^2}{S_\chi}\right) - \left(\frac{(\psi - C_\psi)^2}{S_\psi}\right)\right)} \tag{5}$$

The constant K is included as a way of directly manipulating the intensity of the CO field. This will be used in Section 3 to examine the relationship between field intensity, initial concentration, and survivability.

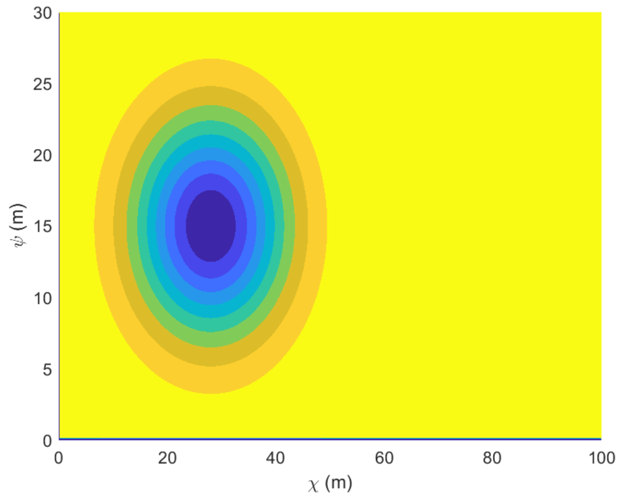

Fig. 1. Top view of the spatial distribution of the field in (5).

2.2 Kinematic equations for single evacuee

Human behavior during an evacuation is complex, and is based on many separate agents' interactions, in addition to their independent trajectories, (Cristiani et al., 2014; Kachroo, 2009). The full dynamics include both translational and rotational motion as well as interaction forces due to collisions, see (Zhou et al., 2018, 2019). For this analysis, only one agent is considered and as such a simplified model can be used. The evacuee's movement can be modelled as a modification to Zermelo's navigation problem (Bryson and Ho, 1975), where the velocities in the χ- and ψ- directions are given below

$$\begin{aligned}\dot{x}(t) &= V(t)\cos(\theta(t)), \\ \dot{y}(t) &= V(t)\sin(\theta(t)),\end{aligned} \tag{6}$$

where $\theta(t)$ is the orientation angle (pose), measured counter-clockwise from the χ-axis. The evacuee speed $V(t)$ is time-varying and depends on both psychological and physiological factors. Physiological factors include the accumulated amount of CO inhaled and the level of fitness of the evacuee; psychological factors include stress and anxiety levels. For simplicity, the speed V here is chosen to be constant and equal to 7 m/s, as proposed in (Demetriou and Kontopyrgos, 2019a) to be the average speed of humans during an evacuation. The solution to (6) provides the position (coordinates $(x(t), y(t))$) of the evacuee with respect to the origin of the reference frame within the spatial domain Ω, taken to be the indoor environment.

2.3 CO Accumulation Modeling

The total amount of CO inhaled along a particular escape path is computed using the line integral of the concentration along the chosen path (Demetriou and Kontopyrgos, 2019a). If the path is denoted by $\mathbf{r}(t) = (x(t), y(t))$ then the line integral (Kaplan, 1984) along this path is defined as a function of θ (control)

$$z(\theta) = \frac{1}{2}\int_\theta c(\mathbf{r})\mathrm{d}s. \tag{7}$$

This is expressed as an explicit function of time as follows

$$\begin{aligned}z(t) &= \frac{1}{2}\int_0^t c(x(\tau), y(\tau))\sqrt{\left(\frac{dx(\tau)}{d\tau}\right)^2 + \left(\frac{dy(\tau)}{d\tau}\right)^2}\mathrm{d}\tau \\ &= \frac{1}{2}\int_0^t c(x(\tau), y(\tau))V(\tau)\mathrm{d}\tau.\end{aligned} \tag{8}$$

When the speed is assumed constant, then the above becomes

$$z(t) = \frac{V}{2}\int_0^t c(x(\tau),y(\tau))\mathrm{d}\tau.$$

The line integral is visualized in Fig. 2. Equation (8) provides

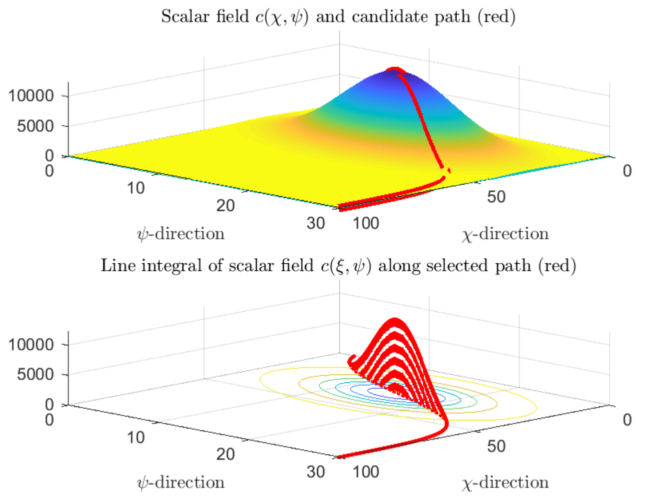

Fig. 2. Line Integral of concentration field $c(\chi,\psi)$ along an escape path for the field in Fig. 1.

the total amount of CO inhaled by the evacuee. The factor of $1/2$ is introduced to model the breathing pattern of a human, wherein only half of the time is spent breathing in and accumulating CO. It represents a simple model in the inhale-exhale cycle which is assumed constant and symmetric. More involved models would have a time-varying fraction, dependent in the CO concentration.

The present suggests the inclusion of an initial concentration $z(0) \neq 0$ due to pre-evacuation psychological freezing. This initial condition may be included in equation (8) as follows

$$z(t) = z(0) + \frac{V}{2}\int_0^t c(x(\tau),y(\tau))\mathrm{d}\tau,$$

or used as a third state variable in (6)

$$\dot{z}(t) = \frac{V}{2}c(x(t),y(t)), \quad z(0) = z_0 \neq 0. \tag{9}$$

Note that z is related to the "evacuee measurement" in (4) via

$$z(t) = z(0) + \frac{V}{2}\int_0^t \gamma(\tau)\mathrm{d}\tau,$$

2.4 Problem statement

The problem can be cast as a variation of the optimal navigation problem where the accumulated amount inhaled $z(t)$ is to be minimized subject to (6). Two related limits are needed: (1) the *instantaneous value* of the CO concentration at the current location of the evacuee $(x(t),y(t))$ given by $\gamma(t)$ in (4) and (2) the *accumulated amount* inhaled up to the current time given by $z(t)$ in (9). The threshold for survivability c_{thresh} is a function of the instantaneous value as presented in (Demetriou and Kontopyrgos, 2019a). Thus, the problem is to ensure that an evacuee reaches any of the exits (X_i,Y_i), $i = 1,\ldots,N$ in the smallest possible time and with the accumulated amount $z(t)$ well below c_{thresh}. The constrained optimization problem becomes that of minimizing the flight time t_f with $(x(t_f),y(t_f)) = (X,Y)$, while ensuring $z((t_f) \leq c_{thresh}$:

$$\text{minimize:} \int_0^{t_f} 1\mathrm{d}t$$

subject to (6), (9) with initial and boundary conditions

$$x(t_0) = x_0,\ x(t_f) = X,$$
$$y(t_0) = y_0,\ y(t_f) = Y,$$
$$z(t_0) = z_0,\ z(t_f) \leq c_{thresh}.$$

The optimal solution has been examined in (Demetriou and Bakolas, 2020) for the 3D case having the 2D case examined here as a special case. This optimal solution is a computationally intensive open-loop solution, which cannot be considered in the context of a real-time human evacuation. Instead, we consider a modification to the level-set guidance presented in (Demetriou and Kontopyrgos, 2019a,b) summarized below.

2.5 Path Planning Algorithms: modified Level-set path planning

The desired path planning algorithm must ensure that the evacuee with initial coordinates $(x(0),y(0))$ follows a path which obeys (6) and which ensures that the accumulated CO, given by (9), remains below the allowable limit c_{thresh} presented in Section 1.3. This will ensure the successful exit of the evacuee. If Θ is defined as the set of paths which satisfy (6), then the optimization problem becomes the selection of the path $\theta(t) \in \Theta$ that ensures that the CO inhaled, given by (9) remains below the limit c_{thresh}.

For the evacuee with initial position $(x(0),y(0))$, Θ is the set of constant-angle paths for the evacuee

$$\Theta = \left\{\theta_j \ : \ \tan(\theta_j) = \frac{Y_j - y(0)}{X_j - x(0)}, \quad \forall j = 1,\ldots,N\right\} \tag{10}$$

with $(X_j,Y_j), j = 1,\ldots,N$ the coordinates of each exit.

The algorithms presented assume there to be no obstructions between the initial position of the evacuee and any of the exits. The inputs to the algorithm shall be the initial location of the evacuee, $(x(0),y(0))$, the coordinates of each of the exits (X_j,Y_j), $j = 1,\ldots,N$, and the CO concentration described in Section 2.1. The algorithms will predict the total accumulated concentration of CO for each admissible path and will then select the one which results in the least accumulated concentration $z(t)$. Algorithm 1 presents the constant-angle algorithm for a single evacuee. It should be noted that Algorithm 1 appears in previous work (Demetriou and Kontopyrgos, 2019a), but is included here for completeness.

The present work adds an initialization step to Algorithm 1, which stipulates that the initial concentration $z(0)$ be nonzero. This is due to the proposed effect of psychological freezing.

Algorithm 1 Constant-angle path based evacuation

1: Using physiological and psychological factors, compute $z(0) \neq 0$
2: Determine evacuee velocity using physiological factors
3: Use (10) generate a set of admissible paths Θ subject to (6)
4: Use (7) with $z(0) \neq 0$ to calculate the accumulated CO over all paths Θ
5: Generate the subset θ_j for which $z(\theta_j) < c_{thresh}$

$$\Theta^{opt} = \{\theta_j \in \Theta \ : \ z(\theta_j) < c_{thresh}\}$$

6: The smallest Θ^{opt} below c_{thresh} is the optimal path

$$\theta^{opt} = \arg\min_{\theta\in\Theta^{opt}} z(\theta),$$

Algorithm 1 may in some cases be unable to generate a feasible path. This suggests a time-varying angle escape path should be used. To ensure the highest chance of survival, a level-set based approach is used (Demetriou and Kontopyrgos, 2019a). Based on Section 1.2, the $2,000$ ppm level set is particularly important to follow. For this algorithm, a constant angle path is followed until the instantaneous CO reaches 2,000 ppm. Subsequently, new angles are generated for each time step to remain on the 2,000 ppm level set. When a path along the line of sight to the exit becomes tangent to the level set, the algorithm follows the new constant-angle path towards the exit. This ensures the peak CO inhaled never exceeds 2,000 ppm, thus allowing for a higher accumulated inhalation and increasing the evacuee's chances of reaching the exit while conscious. Algorithm 2 is presented for the level-set based approach. As with Algorithm 1, Algorithm 2 also includes a nonzero $z(0)$ due to psychological freezing and pre-existing physiological factors.

Remark 1. It should be noted that while following the 2,000 ppm level set is important for ensuring the survivability of a candidate path, it may also be desirable to follow a different level set in the interest of time. Following a level set of 1,000 ppm, for example, would increase survivability at the expense of escape time, while following a 3,000 ppm level set may be more survivable overall due to its time savings. However, the latter comes at the expense of having smaller accumulated threshold of $c_{thresh} = 25,000$ ppm.

Algorithm 2 Level-set based approach

Using physiological and psychological factors, compute $z(0) \neq 0$
Determine evacuee velocity using physiological factors
for time $0 \leq t \leq t_f$ **do**
  if $\gamma(t) < 2{,}000$ ppm **then**
    choose a constant angle path from (10)
    if $z(t)$ >64,000 ppm **then**
      $V = 0$ (death)
    end if
  end if
  if $\gamma(t) > 2{,}000$ ppm **then**
    calculate gradient of CO field ∇c at current location $(x(t), y(t))$
    Using ∇c generate a new θ_{level} at every time step so that the path follows the 2,000 ppm level set

$$\theta(t) = \arctan 2\left(\nabla_x z, \nabla_y z\right) \tag{11}$$

    if $z(t) > 25{,}000$ ppm **then**
      $V = 0$ (death)
    end if
  end if
  At each iteration generate the constant angle path. If the instantaneous peak concentration at the adjacent point is $\gamma(t) > 2{,}000$ ppm then follow the constant angle path.
end for

3. NUMERICAL RESULTS

The two algorithms are implemented over the rectangular domain $\Omega = [0, 100] \times [0, 30]$m for a steady CO field. The field intensity is varied, as is the initial concentration $z(0)$. For the case shown in Fig. 3, the field is of baseline intensity (i.e. $K = 1$). The initial concentration z_0 for this case is zero, which corresponds to no psychological delay.

Figure 3 suggests that Algorithm 2 is much more effective at generating a survivable path than Algorithm 1. Next, the field intensity K is increased until the path generated by Algorithm 2 is no longer survivable. This is shown in Fig. 4. It should be noted that K is varied for simulation purposes only and does not represent a physical constant.

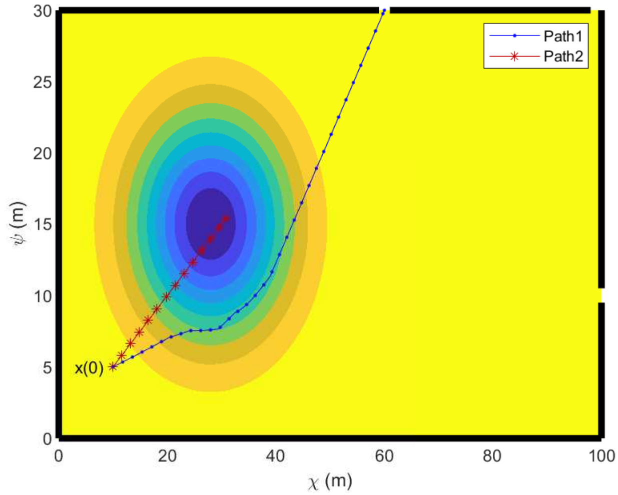

Fig. 3. Escape paths with field intensity $K = 1$ and $z(0) = 0$.

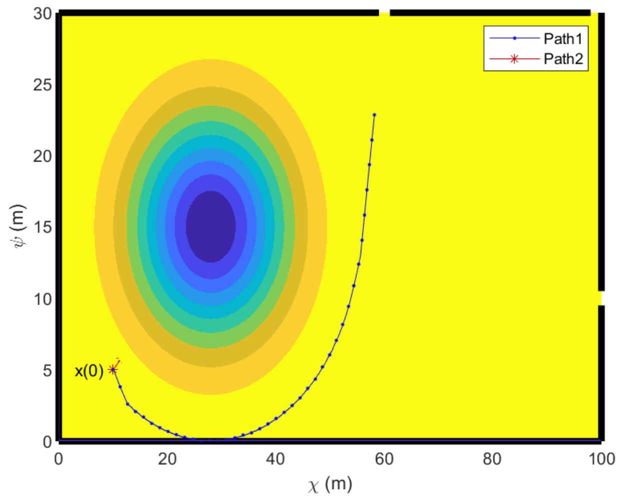

Fig. 4. Escape paths with field intensity $K = 20$ and $z(0) = 0$.

Next, the field intensity K is decreased back to one, and the initial concentration $z(0) \neq 0$ is added. This procedure is followed for initial concentrations of $z(0) = 5,000$ ppm, $z(0) = 10,000$ ppm, $z(0) = 15,000$ ppm, and $z(0) = 20,000$ ppm with any higher than this and the initial concentration itself would incapacitate the evacuee. The results of this are shown in Fig. 5.

The results in Fig. 5 indicate that as the field intensity increases, Algorithm 2 will be less and less able to predict a survivable path. They also indicate that the effectiveness of Algorithm 2 decreases as a function of $z(0)$. This implies that an increased initial concentration renders Algorithm 2 ineffective in overcoming a high field intensity.

This result may be interpreted as a negative correlation between psychological delay and survivability–an intuitive result. Furthermore, the results suggest that $z(0)$ has a greater impact on survivability than does the field intensity, meaning any level-set algorithm which hopes to be successful in guiding human evacuees must take psychological delay into account. It should be noted that this conclusion cannot be drawn for Algorithm 1

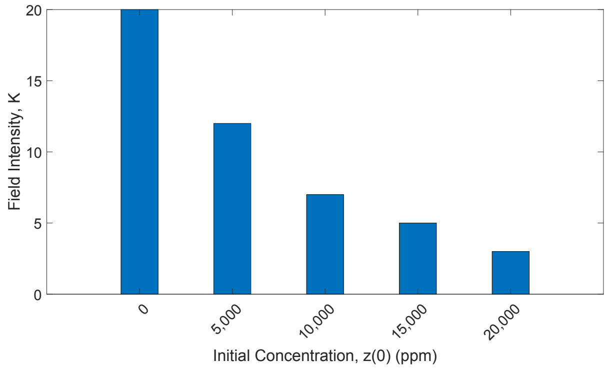

Fig. 5. Intensity K required to render Algorithm 2 unsurvivable.

from these results, because Algorithm 1 was unable to generate a survivable path for any of the field intensities examined.

4. CONCLUSIONS AND FUTURE RECOMMENDATIONS

This work incorporated the psychological effects of pre-evacuation phase in the evacuation planning of humans in indoor environments. The psychological effect of freezing resulted in a non-zero accumulation of the hazardous substance in the evacuee thereby minimizing the options for safe escape.

The present work only considered one evacuee in isolation. Other psychological phenomena that result from the interactions between multiple evacuees will be investigated by the authors in a forthcoming publication. Further psychological traits such as high versus low risk perception and anxiety level will also be considered because they affect the individual's pre-evacuation behavior. Additionally, physiological qualities such as physical fitness will be further examined. Integrating established results on path planning of multi-agent systems with minimal information and the incorporation of obstacles as an additional constraint forms a natural extension to the current work. These extensions with individual and multiple evacuees will appear in a separate forthcoming publication by the authors.

REFERENCES

Arya, S.P. (1999). *Air Pollution Meteorology and Dispersion*. Oxford University Press, New York.

Bryson, Jr., A.E. and Ho, Y.C. (1975). *Applied Optimal Control*. John Wiley & Sons, New York-London-Sydney.

Coşkun, A., Eren, F.A., Eren, e.H., and Korkmaz, l. (2019). Predicting of neuropsychosis in carbon monoxide poisoning according to the plasma troponin, cohb, rdw and mpv levels: Neuropsychoses in carbon monoxide poisoning. *The American Journal of Emergency Medicine*, 37, 1254–1259.

Cristiani, E., Piccoli, B., and Tosin, A. (2014). *Multiscale modeling of pedestrian dynamics*, volume 12 of *MS&A. Modeling, Simulation and Applications*. Springer, Cham.

Demetriou, M.A. and Kontopyrgos, M. (2019a). A level-set based approach for the path planning of human evacuations in contaminated indoor environments. In *Proc. of the 18th European Control Conference*, 1914–1919. Naples, Italy.

Demetriou, M.A. and Kontopyrgos, M. (2019b). A path planning algorithm for human evacuations with an environment dependent motion. In *Proc. of the 58th IEEE Conference on Decision and Control*. Nice, France.

Demetriou, M.A. and Bakolas, E. (2020). Navigating over 3D environments while minimizing cumulative exposure to hazardous fields. *Automatica*, 115, 108859. doi: https://doi.org/10.1016/j.automatica.2020.108859.

Drury, J. and Cocking, C. (2007). The mass psychology of disasters and emergency evacuations: A research report and implications for practice. *Univsersity of Sussex*.

Gozubuyuk, A.A., Dag, H., Kacar, A., Karakurt, Y., and Arica, V. (2017). Epidemiology, pathophysiology, clinical evaluation, and treatment of carbon monoxide poisoning in child, infant, and fetus. *Northern clinics of Istanbul*, 4(1), 100–107.

ICC (2014). *2015 International Wildland-Urban Interface Code*. International Code Council, Country Club Hills, Illinois.

Kachroo, P. (2009). *Pedestrian Dynamics: Mathematical Theory and Evacuation Control*. CRC Press.

Kaplan, W. (1984). *Advanced Calculus*. Addison-Wesley Publishing Company, Reading, MA, third edition.

Kinateder, M., Kuligowski, E., Reneke, P., and Peacock, R. (2015). Risk perception in fire evacuation behavior revisited: definitions, related concepts, and empirical evidence. *Fire Science Reviews*, 4(1), 1–26.

Kuligowski, E. (2017). Burning down the silos: integrating new perspectives from the social sciences into human behavior in fire research. *Fire Mater*, 41, 389–411.

Leach, J. (2004). Why people 'freeze' in an emergency: Temporal and cognitive constraints on survival responses. *Aviation, Space, and Environmental Medicine*, 75(6), 539–542.

Li, G., Zhang, L., and Wang, Z. (2014). Optimization and planning of emergency evacuation routes considering traffic control. *The Scientific World Journal*, 2014, 1–15.

Mu, H.L., Wang, J.H., Mao, Z.L., Sun, J.H., Lo, S.M., and Wang, Q.S. (2013). Pre-evacuation human reactions in fires: An attribution analysis considering psychological process. *Procedia Engineering*, 52(1), 290–296.

National Fire Protection Association, N. (2008). *Fire Protection Handbook*. National Fire Protection Association (NFPA), Quincy, Massachusetts, 20 edition.

Permentier, K., Vercammen, S., Soetaert, S., and Schellemans, C. (2017). Carbon dioxide poisoning: a literature review of an often forgotten cause of intoxication in the emergency department. *Int'l Journal of Emergency Medicine*, 10(1), 14.

Seinfeld, J.H. and Pandis, S.N. (1997). *Atmospheric Chemistry and Physics: From Air Pollution to Climate Change*. Wiley-Interscience, New York.

Vorst, H.C.M. (2010). Evacuation models and disaster psychology. *Procedia Engineering*, 3, 15–21.

Waldau, N., Gattermann, P., Knoflacher, H., and Schreckenberg, M. (2005). *Pedestrian and Evacuation Dynamics*. Springer, Berlin Heidelberg.

Wang, J., Yan, W., Zhi, Y., and Jiang, J. (2016). Investigation of the panic psychology and behaviors of evacuation crowds in subway emergencies. *Procedia Engineering*, 135, 128–137.

Zhao, C.M., Lo, S.M., Liu, M., and Zhang, S.P. (2009). A post-fire survey on the pre-evacuation human behavior. *Fire Safety*, 45, 71–95.

Zhou, M., Dong, H., Zhao, Y., Ioannou, P.A., and Wang, F.Y. (2019). Optimization of crowd evacuation with leaders in urban rail transit stations. *IEEE Transactions on Intelligent Transportation Systems*.

Zhou, M., Dong, H., Zhao, Y., Zhang, Y., and Ioannou, P.A. (2018). Optimal number and location planning of evacuation leader in subway stations. *IFAC-PapersOnLine*, 51(9), 410 – 415. 15th IFAC Symp. on Control in Transportation Systems.